Acta Astronautica 90 (2013) 103–111

Contents lists available at SciVerse ScienceDirect

Acta Astronautica

journal homepage: www.elsevier.com/locate/actaastro

Limits on the use of nuclear explosives for asteroid deflection

Megan Bruck Syal [a,*], David S.P. Dearborn [b], Peter H. Schultz [a]

[a] Brown University, Department of Geological Sciences, 324 Brook St. Box 1846, Providence, RI 02912, USA
[b] Lawrence Livermore National Laboratory, P.O. Box 808 L-16, Livermore, CA 94551, USA

ARTICLE INFO

Article history:
Received 10 January 2012
Received in revised form
15 October 2012
Accepted 16 October 2012
Available online 17 November 2012

Keywords:
Asteroid deflection
NEO mitigation
Planetary defense
Standoff nuclear explosion

ABSTRACT

Recent studies by the US National Research Council identify nuclear explosives as the only current technology able to deflect large asteroids (those exceeding 500 m in diameter) or to mitigate impacts of smaller bodies when the warning time is short. Previous work predicts that either a standoff burst or a very low-yield surface burst is easily capable of deflecting a large (1 km) asteroid without fragmentation. Alternatively, large near-surface or just sub-surface bursts can sufficiently disrupt and disperse smaller bodies (300 m) to ensure that large fractions (in excess of 99.99%) miss the Earth entirely. Even for very short warning times (less than a month), more than 99.5% of a body's mass can be deflected off of an Earth-bound trajectory. However, successfully deflecting a small body, while avoiding fragmentation, becomes a challenging problem when the required kinetic energy increment is a substantial fraction of the body's potential. This paper addresses the challenge of preventing the production of substantial low-speed debris while deflecting small bodies with an impulsive method.

1. Introduction

While payload capabilities of available launch vehicles continue to limit the total mass deliverable to hazardous asteroids or comets, nuclear explosives will remain an important option within the array of proposed hazardous object deflection technologies. At present, nuclear munitions are the only available technology capable of deflecting large bodies. Knowledge of the performance and output of nuclear explosives is assured from an extensive test history, and the deposition of that energy into any material is a well-characterized problem. Any uncertainty in the results of nuclear mitigation resides in our ignorance of the range of structures and material properties that characterize the Near Earth Object (NEO) population. Relatively little quantitative assessment of nuclear deflection has been conducted, and we agree with the letter released by the Office of Science and Technology Policy (OSTP) to the US Congressional Committee on Science and Technology, which concludes, "significantly more analysis and simulation are needed."

With decades of warning, the velocity perturbation required to eliminate an impact is millimeters to a centimeter per second, though a bit more may be desired for a comfortable miss. For large bodies (500 m to 1000 m), the necessary speed change is much less than the 25–50 cm/s escape velocity, and it is reasonable to assume that the impulse providing such small velocity perturbations would not lead to fragmentation or excessive ablation [1,2]. Such requirements have been met in detailed hydrodynamic simulations presented at earlier Planetary Defense Conferences [3,4]; these earlier results on standoff and very low yield surface bursts will be briefly reviewed in the next section.

This situation changes when the approach time is short, particularly when the body is small. With only a few years to impact, the speed change required to deflect a 100 m body approaches the escape velocity, and fragmentation is difficult to avoid. In such a case, a surface burst is capable of sufficiently dispersing a body, so that

* Corresponding author. Tel.: +413 652 9142; fax: +401 863 3978.
E-mail address: Megan_Syal@brown.edu (M. Bruck Syal).

0094-5765/$ - see front matter © 2012 IAA. Published by Elsevier Ltd. All rights reserved.
http://dx.doi.org/10.1016/j.actaastro.2012.10.025

the majority of the material misses the Earth [5,6], greatly reducing the damage potential.

With the clear understanding that nuclear explosives hold a place within the available mitigation technologies, it is desirable to determine the limits of that place. As the outputs of nuclear explosives are well known, the challenge in predicting an asteroid's response lies in the uncertainty of its structures. NEOs are diverse objects with sizes ranging from meters to kilometers and rotation rates ranging from trivial to near break-up. Densities and porosities are highly variable, and shapes range from nearly spherical to elongated, asymmetrical morphologies. There remains much work to determine the optimal use of nuclear explosives against large bodies, for which other technologies are insufficiently robust. Here we present new work on how the nuclear approach can be used to deflect smaller bodies. As the NEO surveys penetrate to substantial completeness at increasingly smaller sizes, it becomes probable that we will have decades of warning for the small to moderate sized bodies that could cause local or regional catastrophe.

2. Earlier work

2.1. Decades to impact

Previously, a series of deflection calculations investigated the response of a spherical, nonporous, inhomogeneous (differentiated into core and mantle with a bulk density of 1.99 g/cm^3) asteroid to the energy deposited by a standoff nuclear burst. CALE, a two-dimensional (2-D) Arbitrary Lagrangian–Eulerian (ALE) hydrocode developed at Lawrence Livermore National Laboratories (LLNL) [7], was utilized for these calculations. The standoff burst's energy was deposited into a thin and tapering set of surface zones (approximately 10 zones deep), across 41° of a hemisphere (half-angle), consistent with a standoff height of 165 m above the surface of the 1 km spherical body. The simulated nuclear explosive was selected for optimized neutron output (high fusion to fission yield), as the cross-section of energetic neutrons is nearly independent of composition for materials between carbon and iron. This results in a penetration depth of 17 g/cm^2, heating substantially more mass than the same flux of x-rays and providing a larger impulse for the same amount of incident energy. Simulations of energetic neutrons incident on granite, which were carried out by MCNP, a general purpose Monte Carlo N-Particle code [8], found that $>70\%$ of the incident energy was deposited (relatively efficient deposition) [9]. Similar simulations on a 1 km body of a different composition found energy absorption efficiencies as high as 75%. Ten kilotons (kt) of energy deposition then converts about 4000 t of surface material into a plasma expanding at over at 2 km/s [3]. An absorption efficiency of 70% was assumed for each calculation in this study.

Tabulated data from the Livermore Equation of State (LEOS) libraries for granite (EOS No. 4030, $\rho=2.63$ g/cm^3), and wet sand (EOS No. 4020, $\rho=1.91$ g/cm^3) were used to describe the hypothetical, differentiated asteroid's rocky core and particulate mantle, respectively. Simulations were run with either no strength or linear strength (compressive strength proportional to the pressure up to the crush pressure, no tensile strength) models; however, for deflection models, strength is unimportant to the results. The models were run until 40 s after deposition, at which point over 97.5% of the body remained bound (Fig. 1) with speeds ranging from 2.2 to 2.4 cm/s. On many orbits, imparting a mere 5 mm/s change in velocity near perihelion and 30 years prior to impact produced a comfortable miss of the Earth.

These simulations did not incorporate a crush curve to treat the energy loss to strong shocks from microporosity. This process is potentially very significant in strong shock regions during early times, which may be shocked to pressures approaching a Megabar. Crushing minimizes any hydrodynamic rebound, and, in the extreme, it limits the momentum pulse to the vaporized material. A series of models run only through this early phase provided speed changes of 0.5–1 cm/s, with $\ll 1\%$ of the material ablated.

In the 2006 Near-Earth Object Survey and Deflection Study by NASA, a new approach for perturbing the orbit of a threatening asteroid was proposed. The idea was to detonate a very low yield nuclear explosive (or explosives) on the surface. These simulations used the same 1 km structures, and the energy was sourced into a 5 m cube at the surface. The 1 kt source easily vaporizes all of the material in the source region, while the 0.1 kt source is near to the lower limit that would be appropriate for an asteroid of this size. The models were run more than 20 s after the burst, in excess of 70 shock crossing times. As expected, a crater was formed, but there was relatively little motion away from the crater.

A 1 kt burst was found to be a bit too large. It posed no danger of fragmenting a 1 km body, but the speed change (2.8 cm/s) and mass ejected (7.5% of the asteroid mass) were far more than required. A 0.5 kt model imparted a speed change of 0.92 cm/s while ejecting 1.9% of the mass, and the 0.1 kt simulation changed the speed by 2.3 mm/s while ejecting less than 0.4% of the mass (Fig. 2). Most of this ejected material had speeds in excess of 10 m/s and, thus, would pass nowhere near the Earth.

Both the standoff and surface burst methods were able to impart a sizable deflection while leaving $\sim$98% of the body bound, assuming only its own weak gravity. The total amount of ejected material depends on the porosity

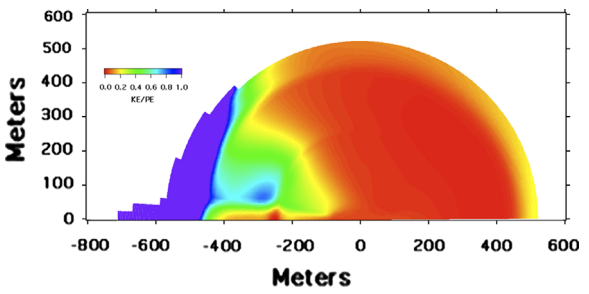

Fig. 1. The ratio of kinetic energy to gravitational potential energy is plotted 40 s after energy deposition. Only the expanded purple region has sufficient kinetic energy to escape from the asteroid. For the models described in Section 2.1, over 97.5% of the body remains bound after 40 s have elapsed. (For interpretation of the references to color in this figure legend, the reader is referred to the web version of this article.)

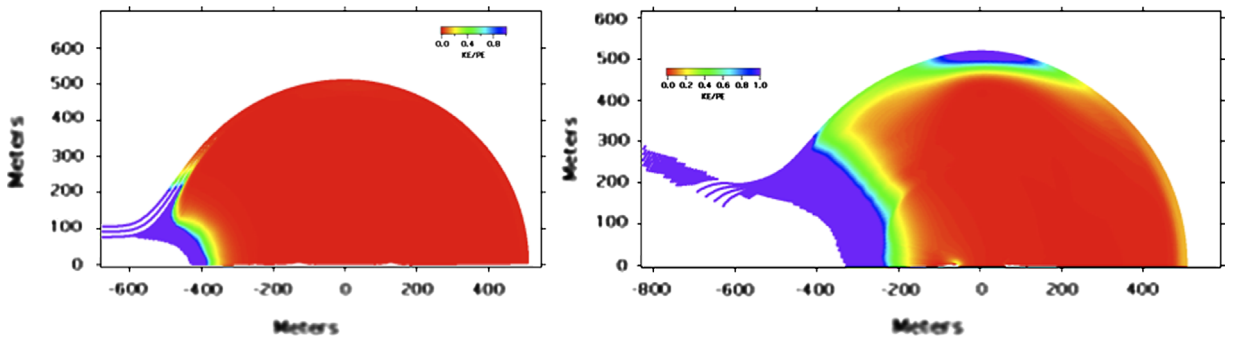

Fig. 2. The ratio of kinetic energy to gravitational potential energy is color-coded for models with a 0.1 kt surface burst (left) and a 1 kt burst (right). The purple material is ejected, though most of the material ejected is outside the printed frames. (For interpretation of the references to color in this figure legend, the reader is referred to the web version of this article.)

of the regolith; dissipative, low-density regolith will not only reduce the mass ejected but also reduce the speed change. While the surface burst approach will clearly work for very low yields, the standoff approach is advantageous in that there is no need to maneuver for a low approach. On the other hand, given the lower yield requirements for a surface burst, a proximity burst with a fuse capable of responding at orbital approach speeds may also be a desirable strategy.

2.2. Years to impact

When the time before impact is short (less than a decade), the necessary speed change becomes a significant fraction of the escape speed, even for large bodies, and fragmentation may be difficult to avoid. If fragmentation occurs near the Earth, allowing a sizable fraction of the material to impact, this can worsen the event. However, if the time to impact and the dispersal speeds are sufficient to cause most of the material to miss the Earth, fragmentation can achieve substantial mitigation, and smaller bodies may be fragmented into pieces unable to penetrate the atmosphere.

Fragmentation was examined for both a 1 km body (about a billion tons) and an Apophis-sized, 270 m body (a bit over 20 million tons). As before, the structures consisted of a higher density core ($\rho = 2.63$ g/cm^3) and a lower density mantle ($\rho = 1.91$ g/cm^3). An equation of state for tuff (soft, porous rock that forms from compacted volcanic ash) was implemented in the mantle region. The bulk density of the structures was 1.99 g/cm^3, close to that measured for asteroid Itokawa ($\rho = 1.95$ g/cm^3) [10]. In order to couple the maximum fraction of the device yields to the asteroids, simulations of surface explosions were conducted. The total energy deposited corresponded to 900 kt within the larger structure and 300 kt within the smaller body. The cylindrical volumes into which energy was initially sourced were approximately 4.5 and 10 m^3 (for the 270 m and 1 km bodies, respectively).

Two-dimensional hydrodynamic modeling of the subsequent explosion led to expanding clouds of debris. The structures were modeled with different strength approximations, including no material strength, a linear strength model (strength proportional to pressure, limited by a

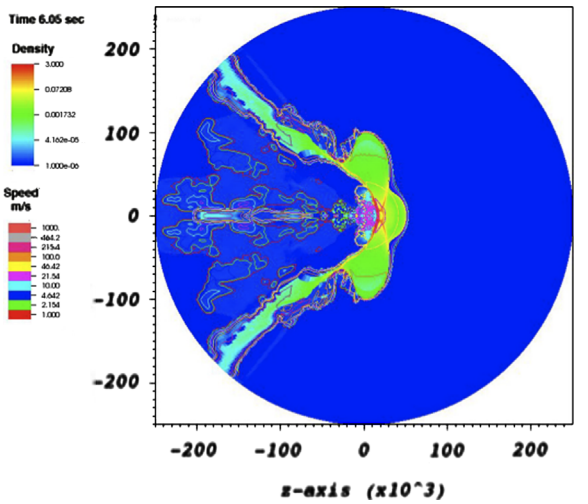

Fig. 3. Density and speed structure of the 270 m body, plotted 6 s after the 300 kt surface burst.

crush strength) often used for shock propagation in rubble, and a model that includes full strength in the core. The yield strength in the core was set to 14.6 MPa, with a shear modulus of 35 MPa. This strength is somewhat weaker than that measured in most granite, and it is near the low end of measured limestone strengths.

The energy source region expands to initiate a shock that propagates through the body, resulting in fragmentation and dispersal. While the material models used have been tested in a terrestrial environment, there are low-density objects, such as Mathilde [11,12], where crater evidence suggests a very porous regolith with efficient shock dissipation. Shock propagation may be less efficient in such porous material, generally reducing the net impulse from a given amount of energy coupled into the surface. More work is needed to understand the limits of very high porosity.

The models were run until the bodies had substantially expanded and the velocity gradients indicated homologous expansion. After about 20 s, fragments from the kilometer-sized bodies had expansion speeds up to 50 m/s. The mass-averaged speeds ranged from 12 to

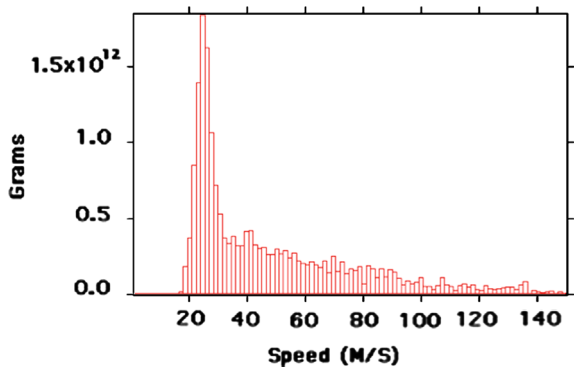

Fig. 4. Speed distribution of the fragments arising from a 300 kt surface burst on a 270 m asteroid. Speeds are plotted 6 s after the explosion.

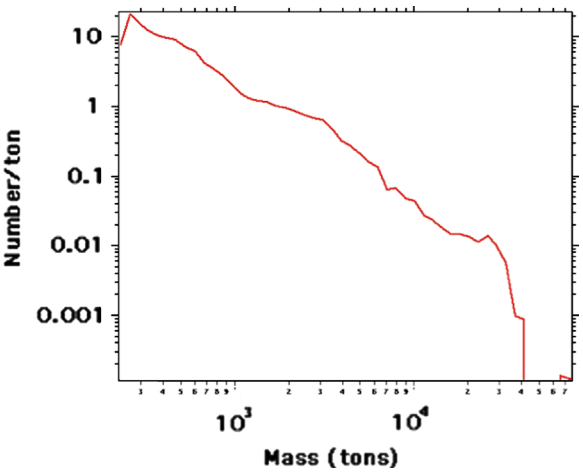

Fig. 5. Mass distribution of the fragments arising from a 300 kt surface burst on a 270 m asteroid.

14 m/s (depending on the model). The smaller body (Figs. 3 and 4) was run with a linear strength model, and, after 6 s, it achieved homologous expansion with a mass-averaged fragment speed near 50 m/s.

The fragment mass distribution for the Apophis-sized model is illustrated in Fig. 5. Here, the number of fragments is proportional to the mass to the power of −1.85; no effort was made to fit the distribution to a theoretical model. These three-dimensional (3-D) fragment distributions were then placed on an impacting trajectory at different times until impact. On this orbit, intercepting an Apophis-sized body only 15–20 days before impact results in tremendous mitigation (Fig. 6). The direction of push is important for such short warning times, and, even when pushing in the least-effective direction, less than 1% of the asteroid's mass would impact Earth for a deflection completed 20 days prior to impact. Even a kilometer-sized object can be effectively dispersed with a Megaton (Mt) class explosive detonated on the surface. However, the smaller dispersal speeds associated with disrupting an asteroid of this size require somewhat earlier

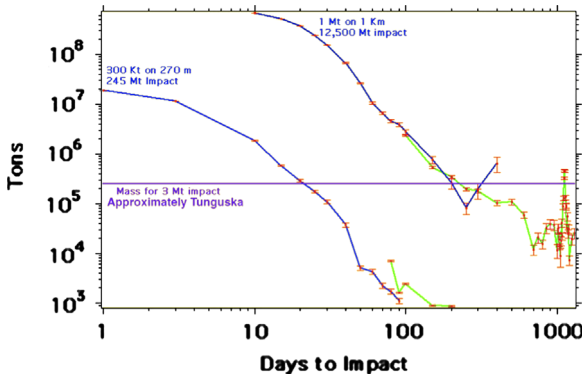

Fig. 6. Total mass remaining a threat to the Earth is plotted as a function of days until impact. The upper line indicates the 1 km body (1 Mt of energy deposited), while the lower line indicates the 270 m body (300 kt deposited). When the original fragment distribution (blue) was too sparse, the fragments were subdivided to a larger number for a better statistical result (green). (For interpretation of the references to color in this figure legend, the reader is referred to the web version of this article.)

fragmentation to achieve success; for a deflection performed a year prior to impact, the cumulative mass from the over 100 impacting fragments would be on the order of the mass delivered during the Tunguska event. None of this material would penetrate the atmosphere.

3. Numerical calculations

Although 3-D radiation/hydrodynamics codes are available for running fully 3-D calculations in a massively parallel environment, here we choose to conserve computational time by using a 2-D code. This initial approach allows for improved spatial resolution and a greater number of simulations to test sensitivity to material properties. CALE is a 2-D Arbitrary Lagrangian Eulerian (ALE) hydrodynamics computer program written in C, allowing both portability and high flexibility in defining complex data structures. CALE has been ported to many machines and is currently developed on DEC Alphas, Linux platforms, Windows, and Mac OS X. The physics algorithms and approximations incorporate a wide variety of ideas and techniques developed by many different people at LLNL over the last 30 years.

CALE generally follows the basic structure of the astrophysics ALE hydro code written by Barton under the guidance and oversight of LeBlanc and Wilson [7]. The Lagrange phase of CALE generally follows the work of Wilkins' HEMP code [13]. The 2-D artificial viscosity comes from the work of Schulz, Christensen, and Tipton. The anti-hour glassing filter comes from the work of Margolin on the CONCHAS-SPRAY code of LANL [14]. The ALE grid motion algorithms stem from the basic work on equipotential grids done by Winslow and Crowley [15] and elaborations by Barton, LeBlanc and Tipton. The original advection scheme of Barton, LeBlanc and Wilson has been modified to include the basic monotonicity ideas of Van Leer, with further elaborations by Christensen. The "volume fraction" method for Eulerian interface tracking was developed by LeBlanc and Wilson and extensively

modified by Tipton. The discontinuous velocity slide line treatment was developed by Barton. The energy diffusion and magnetic diffusion algorithms draw on the work of Winslow, as elaborated by Tipton [16].

The thermal diffusion package uses a two-temperature model, consisting of separate matter and radiation temperatures, which permits thermal heat conduction and radiation diffusion to be modeled concurrently. Electrons and ions are assumed to be described by a Maxwellian distribution and to be in thermodynamic equilibrium with each other; the radiation field is assumed to possess a Planckian distribution. When thermal conduction is considered in the absence of radiation diffusion, the radiation temperature is numerically "clamped" to the matter temperature and the model effectively becomes a one-temperature model. With these assumptions, the amount of radiant energy that is spatially transported from zone to zone is controlled by the Rosseland mean opacity. The rate at which energy is exchanged between the matter energy field and the radiation energy field is controlled by the Planck mean opacity. In the case of thermal conduction, a conductive opacity is used to produce the correct spatial transport of the thermal energy, while a Planck opacity of near infinity clamps the radiation temperature to the matter temperature.

Past deflection simulations with CALE, as described in Section 2, did not include any porosity within the material models. However, the currently available bulk density measurements for asteroids suggest that many of these objects contain significant void space. Although the effects of both microporosity (voids between individual grains) and macroporosity (voids between larger boulders) may contribute to the low bulk densities observed for asteroids, a role for microporosity is strongly suggested. For example, given a 270 m-diameter asteroid of moderate microporosity ($\Phi=0.16$), a fully dense version of this asteroid would require a total macroscopic void space equal to the volume of a 146 m diameter, spherical cavity. Results from impact experiments into microporous targets have also been used to explain both the peculiar style and distribution of impact craters at Mathilde [12] and the evolution of the Deep Impact cratering event [17]. Hence, while the effects of larger-scale voids within rubble pile-type bodies are an important consideration, asteroids are also likely to possess non-negligible microporosities. Due to the geometrical limitations of a 2-D model (a rubble pile structure would not be well-described by a spherically symmetric body), this work focuses on microporosity effects.

An experimentally determined crush curve for 16% porous Ste. Genevieve Limestone ($\rho=2.27$ g/cm^3) was implemented using the EOS option for a user-defined porosity model in CALE. A table of pressure–density pairs ranging from $\rho=2.27$ g/cm^3 ($\Phi=0.16$) to $\rho=2.70$ g/cm^3 (fully dense limestone, $\Phi=0.0$) defines the Hugoniot below a critical pressure; once the limestone is fully compacted, it is described by a Grüneisen EOS for non-porous Lynchburg limestone (Eq. 1):

$$P=\frac{\rho_0 c^2 \mu\left[1+\left(1-\frac{\gamma_0}{2}\right)\mu\right]}{\left[1-(S_1-1)\mu\right]^2}+\gamma_0 E \quad (1)$$

Where $\rho_0=2.70$ g/cm^3 (reference density), $\mu=(\rho/\rho_0-1)$, $c=0.45$ (vertical intercept of the $Us-Up$ shock Hugoniot), $S_1=1.4$ (slope of the $Us-Up$ shock Hugoniot), $\gamma_0=1.0$ (Grüneisen gamma at reference density), P is the pressure, and E is the internal energy.

Previous work [18] has detailed the use of these limestone equations of state for hypervelocity impact simulations. Although the simulations described in [18] employed a different hydrocode (GEODYN, a Godunov-based Eulerian code), benchmark tests demonstrate that shock propagation through geological materials (from a sourced energy deposit) is nearly identical between CALE and GEODYN. Hence, the particular material models used in this work have been well-benchmarked for use in CALE, particularly with asteroid deflection simulations.

4. Results and discussion

As discussed in the introduction, large bodies (500–1000 m) with escape speeds of 25–50 cm/s can be given an impulse sufficient to induce a miss (~1 cm/s) with essentially no danger of fragmentation; this becomes increasingly difficult as asteroid size declines. For a 100 m asteroid, the escape speed is near 5 cm/s, and inducing a 1 cm/s speed change will almost certainly result in extensive debris ejection or fragmentation. Fortunately, kinetic impactors can address bodies of this size, and a series of smaller speed changes can also be implemented to avoid undesirable fragmentation. Even with this strategy, there is a concern that the cumulative ejecta may become a large fraction of the body's mass. As was shown in [5,6], robustly fragmenting a body creates a debris field so extended that the remaining threat to the Earth is minimal. This is not true if the body is barely disrupted such that a concentrated debris field is still on a collision path. On such small bodies, if impactors failed or if the time is short, deflection via the nuclear option would be very difficult, and robust fragmentation by nearby high yield burst should be considered.

The Apophis-sized body is near the boundary at which impactor deflection missions become heroic and nuclear deflection might be considered. We have performed a series of calculations in which a standoff source of high-energy neutrons heat the surface of a 270 m homogeneous sphere. Models were implemented with a density associated with non-porous Lynchburg Limestone ($\rho=2.70$ g/cm^3), as well as a crush curve and density from a 16% porous Ste. Genevieve Limestone ($\rho=2.27$ g/cm^3). The masses of the higher density models were 27.8 million tons, while the porous models were 23.4 million tons. An energy absorption efficiency of 70%, derived in previous investigations of neutron deposition [8], was assumed for all calculations.

The first pair of simulations modeled approximately 70 kt of neutron output originating 60 m from the surface of the body. This directly irradiates the asteroid's surface with about 17 kt of energy (11.9 kt of total absorbed energy) in the surface, significantly more than the energies used to deflect 1 km bodies in previous work. The ratio of the kinetic energy to potential energy (KE/PE) at approximately 6 s after the 70 kt burst is plotted in Fig. 7. The non-porous body has KE/PE > 1.0 and is completely

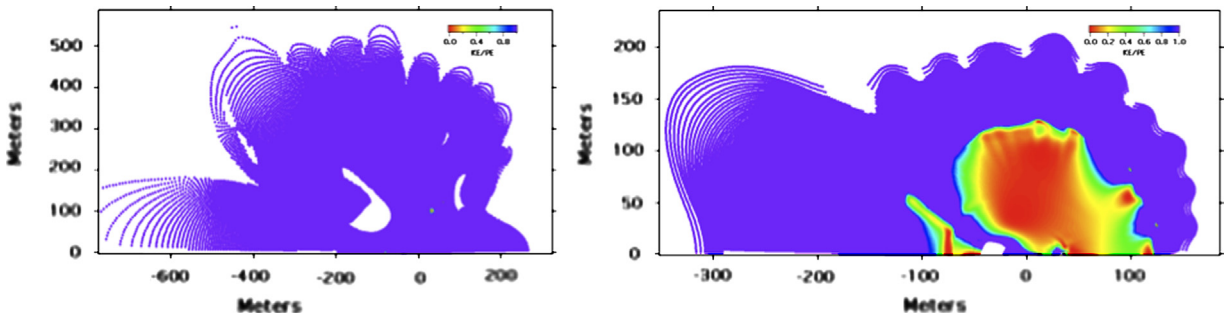

Fig. 7. Kinetic to potential energy ratios for the non-porous (left) and porous (right) asteroid models, plotted 6 s after a 70 kt standoff burst (HOB=60 m). Material with speeds above escape velocity appears purple; green through red material has insufficient kinetic energy to escape the gravitational potential. (For interpretation of the references to color in this figure legend, the reader is referred to the web version of this article.)

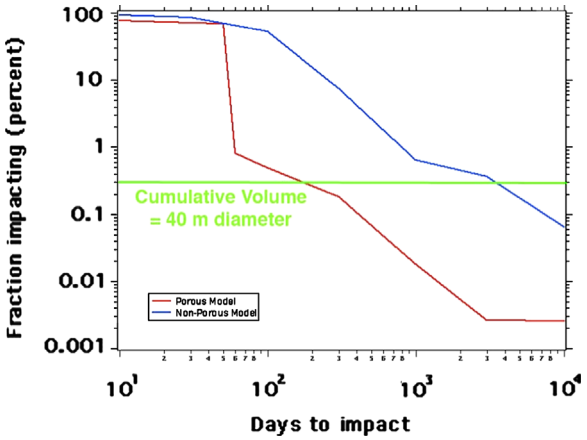

Fig. 8. The percentage of the asteroid's total mass that will impact Earth for both the porous (red) and non-porous (blue) cases is plotted as a function of days until impact (70 kt burst). (For interpretation of the references to color in this figure legend, the reader is referred to the web version of this article.)

fragmented. In the porous body, more than 65% of the material is nominally bound and is expected to coalesce. The momentum in this bound material provides a speed change of several centimeters per second. Propagating the bound piece and individual fragments from these models along an orbit ($a\sim2$ AU, $e\sim0.5$), shows that the porosity actually provided a superior result (Fig. 8).

The fragmented (non-porous) model was weakly dispersed, and, even after 100 days, most of the material would still impact the Earth. The speed increment associated with the bound portion of the porous model resulted in a successful miss by this material after only 60 days. With earlier dispersal, the debris field of the ejected material expands at about the same rate as the non-porous model, but as the mass fraction of the debris is smaller, the cumulative impacting material is below that of Tunguska after only 200 days (Fig. 8). This pair of simulations shows that a 70 kt yield is too high for this height of burst (HOB) on a 270 m body and demonstrates that we can recover the weakly fragmented case that should be avoided. It also provides the interesting result that, in an energy rich environment, porosity can actually improve the odds of a successful deflection. In the absence of a characterization mission, and with the need for a strong push, assuming non-porous is the conservative choice.

This next pair of models reduced the source yield to 7.0 kt at the same 60 m HOB, such that 1.70 kt irradiates the surface of the asteroid (1.19 kt of total absorbed energy). By maintaining the burst height, the energy heated the same azimuthal region as the previous calculation. The amount of material that was still nominally bound was between 60 and 65% in both the porous and non-porous models (Fig. 9). The coalesced pieces of the non-porous model had higher speed, missing Earth after only 20 days of flight, but even the large piece of the porous model missed by 60 days (Fig. 10). Here the time for the cumulative volume of the threatening fragments to drop below a Tunguska-sized event is about 300 days.

For a simple deflection, the 7.0 kt yield is still too high (or, alternatively, the HOB too low). Stepping down again in yield, models were run for a 0.5 kt burst detonated at a 60 m HOB (0.0852 kt of total absorbed energy). Most of the material ($>99.7\%$ of the body) remained bound in this case (Fig. 11). The speed change imparted to the bound portion was ~3 mm/s for the nonporous case and just ~1 mm/s for the porous case. While these deflection velocities may be appropriate for situations involving relatively large warning times (decades), the factor of three difference in asteroid response between the non-porous and porous cases illustrates the importance of quantifying a body's material properties prior to deploying an impulsive deflection method. In addition, it should be noted that the porosities of many asteroids greatly exceed the modest value of $\Phi=0.16$ used in this study [19], which was limited by the availability of experimental crush curve data.

For this last 0.5 kt yield case, it is instructive to compare the calculated velocity change (δv) with an estimate derived from an analytical approach to the problem. An approximate expression for a standoff burst-delivered velocity change is $\delta v=0.1Ay/D^3$, where y is total neutron yield in kt (here, 0.35 kt), A represents a dimensionless efficiency factor (here, ~0.3), D is asteroid diameter in km (0.27 km), and δv is deflection velocity in cm/s [20]. For these parameters, $\delta v\sim5.33$ mm/s, a slightly larger impulse than the numerical results obtained in this study for the nonporous asteroid ($\delta v\sim3$ mm/s). The

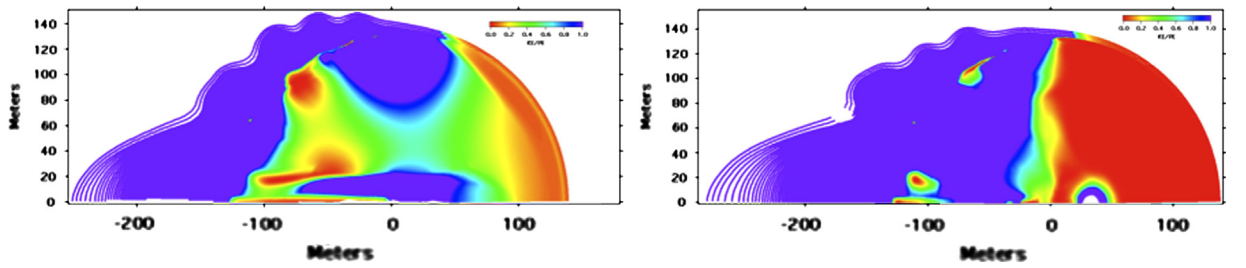

Fig. 9. For a 7.0 kt standoff burst, the non-porous (left) and porous (right) models showing material with speeds above escape velocity (purple) and material with insufficient energy to escape the gravitational potential (green through red). (For interpretation of the references to color in this figure legend, the reader is referred to the web version of this article.)

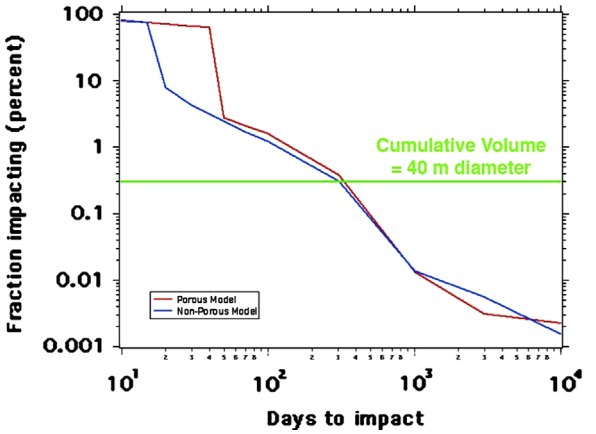

Fig. 10. The percentage of the asteroid's total mass that will impact Earth for both the porous (red) and non-porous (blue) cases is plotted as a function of days until impact (7.0 kt burst). (For interpretation of the references to color in this figure legend, the reader is referred to the web version of this article.)

disparity between the analytical approximation and the numerical results increases for the porous case ($\delta v \sim 1$ mm/s).

Previous work to quantify the effects of asteroid porosity on standoff nuclear burst deflection employed a 1-D hydrocode and used an ANEOS equation of state for granite, combined with a p-alpha porosity model with $\Phi = 0.5$ [21,22]. This approach contrasts with the present study in three principal ways: the use (here) of an empirically derived porosity model, the use of a lower porosity ($\Phi = 0.16$), and the ability to quantify 2-D geometrical effects on the propagation of shock waves through the asteroid. The 1-D approach calculated momentum impulses per unit area as a function of initial specific energy [21]. For relatively large specific energies (greater than several MJ/kg), the difference between porous and non-porous momentum transfer was comparable to the factor of three difference found in our calculations. However, it is important to note that our simulations used much lower specific energies, on the order of $\sim 10^{-2}$ MJ/kg, as we were deflecting a smaller body (270 m-diameter, as opposed to the 1 km-diameter case in [21]). For specific energies in this range, the results of [21] suggest a much larger change in momentum impulse per unit area (approximately two orders of magnitude difference between porous and nonporous) than the factor of three results reported here. These differences may be attributable to a combination of factors, including: different material models, different initial porosities, and 1-D vs. 2-D code effects.

Lastly, it should be emphasized that the results of any hydrocode simulation are necessarily dependent on the equations of state and constitutive models used. For the case of any hypothetical, hazardous object, a significant amount of uncertainty in its composition and internal structure will be intrinsic to the problem. Hence, for numerical simulations of asteroid deflections, the results depend upon certain assumptions made in regards to material models. In addition, the development of relations that accurately describe the response of geologic materials to the extreme pressure and temperature conditions of these deflection problems is a very active area of research in its own right. The intention of this study is not to provide absolute device yields and standoff distances to be deployed in specific cases but to better quantify the sensitivity of a given asteroid to any assumptions about its porosity. Many more simulations are necessary to fully capture the range of material model-dependent effects on impulsive deflection methods.

5. Conclusions

Nuclear explosives comprise the only present technology capable of deflecting the most catastrophic threats (>500 m) with a sufficient change in velocity to avert disaster. In the case of smaller bodies, if alternate methods fail or the warning time is too short, the nuclear option provides considerable mitigation when used only a few years prior to impact. Even for larger bodies, the payload mass necessary for a successful nuclear burst-driven deflection is well within current launch vehicle capabilities.

We have now extended earlier simulations of nuclear deflection to examine the challenges of a smaller body and potentially shorter warning times (years). We have also included microporosity to begin to determine when this material property is a sensitive uncertainty. We find that a modest yield standoff burst can fragment a non-porous rubble structure, but that 16% porosity resulted in a substantially bound body. This result demonstrates that the non-porous case presents the highest risk of fragmentation, but it also suggests that robustly fragmenting

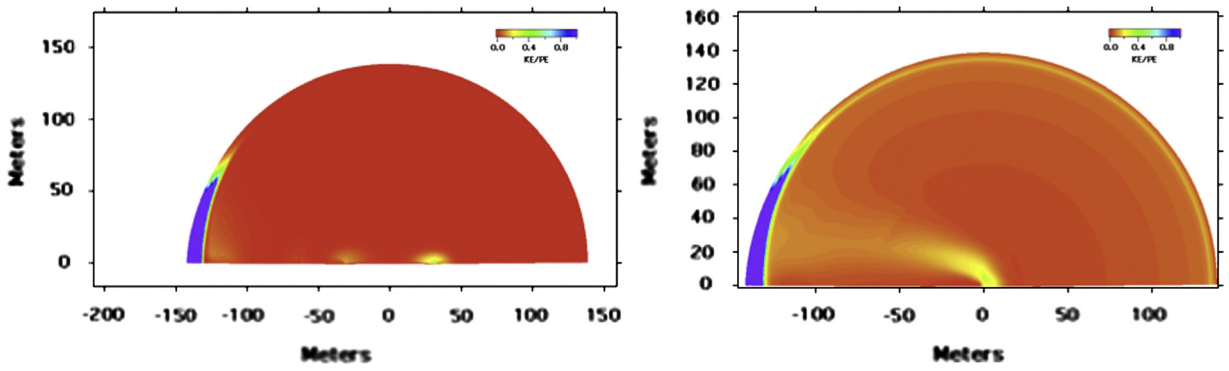

Fig. 11. Kinetic to potential energy ratios for the non-porous (left) and porous (right) cases after a 0.7 kt burst. Less than 1% of the material is ejected (purple). (For interpretation of the references to color in this figure legend, the reader is referred to the web version of this article.)

smaller bodies can be accomplished by high yield standoff bursts, a strategy which reduces the extra mass requirements associated with rendezvous missions. This is an approach that we will study in more detail in the future. Interestingly, even when copious material is ejected, as long as the remaining bound material is imparted with a reasonable speed change, the mitigation against an Apophis-sized object can be substantial (when done a year before impact). Alternatively, very low yields or large heights of burst can deflect bodies of this size when there are decades to impact.

Despite NEO structural and compositional uncertainties, detailed simulations show that nuclear explosives will provide considerable protection. While their use to perturb a body some decades out remains the more desirable option, fragmenting the body remains a viable back-up option with only a few years of lead-time.

Acknowledgments

This work performed under the auspices of the US Department of Energy by Lawrence Livermore National Laboratory under contract DE-AC52-07NA2734.

References

[1] T.J. Ahrens, A.W. Harris, Deflection and fragmentation of near-Earth asteroids, Nature 360 (1992) 429–433.
[2] J.C. Solem, Deflection and disruption of asteroids on collision course with Earth, J. Br. Interplanet. Soc. 53 (2000) 180–196.
[3] D.S.P. Dearborn, 21st century steam for asteroid mitigation, Technical Report UCRL-PROC-202922, LLNL, 2004.
[4] D.S.P. Dearborn, S. Patenaude, R.A. Managan, The use of nuclear explosives to disrupt or divert asteroids, Technical Report UCRL-PROC-228569, LLNL, 2007.
[5] B. Wie, D.S.P. Dearborn, Earth-impact modeling and analysis of a near-Earth object fragmented and dispersed by nuclear subsurface explosions, 20th AAS/AIAA Space Flight Mechanics Meeting (2010) AAS 10–137.
[6] B.D. Kaplinger, B.Wie, D.S.P. Dearborn, Efficient parallelization of nonlinear perturbation algorithms for orbit prediction with applications to asteroid deflection, 20th AAS/AIAA Space Flight Mechanics Meeting (2010) AAS 10–225.
[7] R.T. Barton, Development of a multimaterial, two-dimensional, arbitrary Lagrangian-Eulerian mesh computer program, in: J.M. Centrella, J.M. LeBlanc, R.L. Bowers (Eds.), Numerical Astrophysics, Jones & Bartlett, Boston, 1985, pp. 482–497.
[8] P.J. Bedrossian, Neutrons and Granite: Transport and Activation, Technical Report UCRL-TR-203529, LLNL, 2004.
[9] MCNP-A General Monte Carlo N-Particle Transport Code, Version 5, LANL document LA-UR-03–1987, 2003.
[10] S. Abe, T. Mukai, N. Hirata, O.S. Barnouin-Jha, A.F. Cheng, H. Demura, R.W. Gaskell, T. Hashimoto, K. Hiraoka, T. Honda, T. Kubota, M. Matsuoka, T. Mizuno, R. Nakamura, D.J. Scheeres, M. Yoshikawa, Mass and local topography measurements of Itokawa by Hayabusa, Science 312 (2006) 1344–1347.
[11] C.R. Chapman, W.J. Merline, P.C. Thomas, Cratering on Mathilde, Icarus 140 (1999) 28–33.
[12] K.R. Housen, K.A. Holsapple, M.E. Voss, Compaction as the origin of the unusual craters on the asteroid Mathilde, Nature 402 (1999) 155–157.
[13] M.L. Wilkins, Calculations of elastic-plastic flow, in: B.J. Alder, S. Fernbach, M. Rotenberg (Eds.), Methods in Computational Physics, III, Academic Press, 1964, pp. 211–263.
[14] L.D. Cloutman, J.K. Dukowicz, J.D. Ramshaw, and A.A. Amsden, CONCHAS-SPRAY: A computer code for reactive flows with fuel sprays, Technical Report LA-9294-MS, LANL, 1982.
[15] A.M. Winslow, Equipotential zoning of two dimensional meshes, Technical Report UCRL-7312,, LLNL, 1963.
[16] R.E. Tipton, A 2D Lagrange MHD code, in: C.M. Fowler, R.S. Caird, D.J. Erickson (Eds.), Proceedings of the Fourth International Conference on Megagauss Magnetic Field Generation and Related Topics, Plenum Press, 1987, pp. 299.
[17] P.H. Schultz, C.A. Eberhardy, C.M. Ernst, M.F. A'Hearn, J.M. Sunshine, C.M. Lisse., The Deep Impact oblique impact cratering experiment, Icarus 191 (2007) 84–122.
[18] T.H. Antoun, L.A. Glenn, O.R. Walton, P. Goldstein, I.N. Lomov, B. Liu, Simulation of hypervelocity penetration in limestone, Int. J. Impact Eng. 33 (2006) 45–52.
[19] D.T. Britt, D.K. Yeomans, K.R. Housen, G. Consolmagno, Asteroid density, porosity, and structure, in: W.F. Bottke Jr., A. Cellino, P. Paolicchi, R.P. Binzel (Eds.), Asteroids, III, University of Arizona Press, Tucson, 2002, pp. 485–500.
[20] T.J. Ahrens, A.W. Harris, Deflection and fragmentation of near-Earth asteroids, in: T. Gehrels (Ed.), Hazards Due to Comets and Asteroids, University of Arizona Press, Tucson, 1994, pp. 897–927.
[21] K.A. Holsapple, On nuking menacing asteroids, Lunar and Planetary Institute Science Conference Abstracts, 34, (2003) 1799.
[22] K.A. Holsapple, About deflecting asteroids and comets, in: M.J.S. Belton, T.H. Morgan, N. Samarasinha, D.K. Yeomans (Eds.), Mitigation of Hazardous Comets and Asteroids, Cambridge University Press, Cambridge, 2004, pp. 113–140.

Megan Bruck Syal is currently a Ph.D. candidate in the Department of Geological Sciences at Brown University (Providence, RI). In 2007, she obtained B.A.'s in Astrophysics and Mathematics from Williams College (Williamstown, MA). After working in the Director's Office of the Chandra X-ray Center (Cambridge, MA) for 2 years, she commenced her graduate studies at Brown in 2009. In addition to NEO mitigation, her research interests include experimental studies of impact-generated vapor plumes and geological processes at small solar system bodies. She is currently a NASA Earth and Space Science Fellow and a member of the Deep Impact Extended Investigation (DIXI) Science Team.

Dr. David S. P. Dearborn is a graduate of UCLA (1970) and the University of Texas at Austin (1975). He has held positions at the Copernicus Institute in Warsaw, the Institute of Astronomy in Cambridge, The California Institute of Technology, and Steward Observatory in Tucson. He is currently a research physicist at the Lawrence Livermore National Laboratory. His astrophysical research includes theoretical studies on the physics of stars, observations of isotope ratios in red giants, and the discovery of several short period variables. His current research on the diversion of asteroids by nuclear explosives mixes his skills in astrophysics and nuclear weapons effects.